

Tuning Tidal Turbines In-Concert to Maximise Farm Efficiency

ROSS VENNELL †,

Ocean Physics Group, Department of Marine Science, University of Otago, New Zealand

(Received Monday 29th November, 2010 07:45 and in revised form ??)

Tuning is essential to maximise the output of turbines extracting power from tidal currents. To realise a large fraction of a narrow channel's potential, rows of turbines not only have to be tuned for a particular tidal channel, they must also be tuned in the presence of all the other rows, i.e. "tuned in-concert". The necessity for in-concert tuning to maximise farm efficiency occurs because the tuning of any one row affects a channel's total drag coefficient and hence the flow through all other rows. Surprisingly in several circumstances the optimal in-concert tunings are the same or almost the same for all rows. Firstly, in both constricted and unconstricted channels, rows with the same turbine density have the same optimal tuning. Secondly turbine rows in channels with a quasi-steady dynamical balance typically have almost the same optimal in-concert tunings, irrespective of their turbine density or any channel constrictions. Channel constrictions, occupying a large fraction of the cross-section or adding more rows of turbines also make optimal tunings more uniform between rows. Adding turbines to a cross-section increases a farm's efficiency. However, in a law of diminishing returns for quasi-steady channels, turbine efficiency (the output per turbine) decreases as turbines are added to a cross section. In contrast for inertial channels with only moderate constrictions turbine efficiency increases as turbines are added to a cross-section.

1. Introduction

Power generation from tidal currents can contribute to the need for renewable energy sources, with the high flows through narrow tidal channels having the greatest potential for power generation (e.g. Sutherland *et al.* 2007). While single tidal turbines will contribute to energy generation, making a significant contribution will require densely packed channels which may contain hundreds of turbines. On this scale power extraction enhances drag and retards flow along a channel, which limits its potential (Garrett & Cummins 2005, hereafter GC05). This work focuses on how the number and placement of turbines within a farm determine the fraction of a channel's potential which is available for power production, i.e. farm efficiency.

Turbine tuning is critical to maximising the power available and is typically done by adjusting blade pitch. To maximise the power from the classic Lanchester-Betz actuator disc model of a turbine, the flow through the turbine must be tuned to be $2/3$ of the free stream flow (Lanchester 1915, Betz 1920). The Lanchester-Betz model is for an isolated turbine, far from any boundaries or other turbines. To realise a significant fraction of a tidal channel's potential turbines must be densely packed within the confines of the channel. As a result they must also be tuned for a particular channel, tidal forcing and turbine density (Vennell 2010, hereafter V10). This work addresses the novel idea that to maximise farm efficiency rows of turbines not only need to be tuned for a particular

† Dept. Marine Science, University of Otago, Dunedin 9056, NZ, ross.vennell@otago.ac.nz

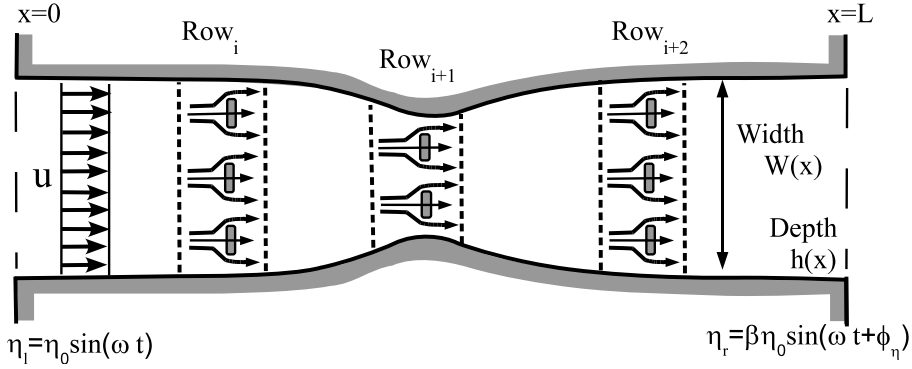


FIGURE 1. Schematic of a constricted tidal channel with rows of turbines and a rectangular cross-section.

channel, they must also be tuned in the presence of other rows, i.e. “tuned in-concert”. The primary aim of this work is to improve understanding of how farm efficiency is affected by tuning and turbine density as a farm grows from a single classic isolated Lanchester-Betz turbine extracting power from the flow’s kinetic energy, to a large farm extracting energy from head loss across the turbines.

GC05 used a simple model to estimate the potential to generate power from tidal currents along a channel, figure 1. The model was the first to allow fully for the enhancement of the channel’s gross drag coefficient due to power extraction, which slows the macroscopic flow along the channel. As a result there is an optimal gross farm drag coefficient which gives the maximum possible power which can be lost by the flow to the turbines, i.e. a channel’s potential to produce power. GC05’s estimate of potential assumes that turbines occupy the entire cross-section of a channel. In most channels gaps between turbines will be essential to allow for navigation of vessels and marine life. The mixing of the enhanced flow through the gaps with the slower flow through the turbines results in an additional loss which cannot be turned into electricity (Garrett & Cummins 2007, hereafter GC07). As a result of this wake mixing loss, figure 2, there is a distinction between a channel’s potential, which is the maximum power which can be lost by the flow to the turbines, and the smaller power available for electricity production. GC07 showed that at most 2/3 of the power lost to the turbines was available for power production. This required that turbines be tuned to the same through flow as the classic isolated Lanchester-Betz turbine and that they occupy as small a part of the cross-section as possible.

GC07 assumed that the free stream flow was fixed, i.e. there is no interaction between drag due to the turbines and strength of the flow along the channel. However, for a tidal channel driven by a given headloss between its ends the flow is not fixed but is affected by the farm’s gross drag coefficient (GC05). The farm’s drag coefficient depends on the tuning of the turbines within it, thus for tidal channels the macroscopic along channel flow is a function of turbine tuning (V10). V10 showed that this interaction between the tuning and the flow requires turbines to be tuned for a particular tidal channel and turbine density in order to maximise the power available. V10 also found that, even with gaps between turbines, it is possible to realise most of a channel’s potential using optimally tuned turbines. To achieve this with the fewest turbines they must fill most of the channel’s cross-section. If it is not possible to fill a large fraction of the cross-section then many rows of optimally tuned turbines can also realise most of a channel’s potential.

The channels considered by V10 had a uniform cross-section and rows containing the same number of turbines. However many channels vary in width, e.g. have constrictions which may be targeted for power generation. Also, practical considerations, e.g. proximity of settlements or sensitive areas, may mean rows must have different numbers of turbines. Rows spread along a channel with a variable cross-section or rows which have different numbers of turbines will likely require different tunings to maximise their power available. Going a step further, rows interact with each other even if they are widely enough spaced that any flow disturbance due to a row is fully mixed before the flow encounters the next row. This interaction occurs because the tuning of any one row affects the channel's total drag coefficient. In turn, the total drag coefficient influences the strength of the flow along the entire channel. Thus the tuning of any one row alters the flow through all rows and hence affects the power production of all rows. Consequently to maximise the total power available from a farm in a channel each turbine row must be tuned in the presence of all the other rows to find an optimal set of tunings, i.e. require tuning in-concert. This work develops a simple 1D model which can be used to find this set of tunings and explores optimal in-concert tunings for rows of turbines in channels with constrictions and/or where the cross-sectional density of turbines varies between rows.

A secondary aim of this work is to provide understanding for developers using 2D and 3D hydrodynamical tidal models to assess the tidal current resource potential of a particular channel. To model the effects of turbines on the macroscopic flow modellers will need to incorporate idealised turbines into their models (V10). At the high turbine densities required to realise a large fraction of a channel's potential these idealised turbines will need to be tuned in-concert. In the complex geometries of the hydrodynamical models each turbine may need to be individually tuned in-concert with all other turbines. Thus N turbines may need to be optimised within a N dimensional tuning space. With 2D and 3D hydrodynamical models taking many hours per model run to evaluate a single set of tunings, finding the optimal in-concert tunings for a large number of turbines may be computationally prohibitive. Thus a secondary aim is to provide results and understanding from a simple model that will allow developers to efficiently search their large tuning space.

2. Model

2.1. Variable cross-section channel model dependent on farm drag coefficient

GC05's model for turbines in a tidal channel connecting two large water bodies is adapted for multi-row turbine farms. Consider a shallow narrow tidal channel with a variable rectangular cross-section of area $A(x) = W(x)h(x)$ that connects two large water bodies, figure 1. The channel has rows of turbines distributed along its length. Tidal currents are driven through the channel by the difference in surface elevation, η , between the water bodies and currents are assumed uniform across the narrow channel. The starting point for the channel model is the depth averaged 1D shallow water momentum balance

$$\frac{\partial u}{\partial t} + u \frac{\partial u}{\partial x} = -g \frac{\partial \eta}{\partial x} - \frac{C_D}{h} |u|u - F \quad (2.1)$$

where $u(x, t)$ is the along channel velocity, $\eta(t, x)$ is the displacement of the water's free surface (assumed small compared to the water depth h), C_D is the drag coefficient for bottom friction and $F(x, t)$ is the additional drag due to power extraction by the turbines. It is assumed that the channel is short enough that the transport does not vary along the channel. Vennell (1998) derived conditions for channels with a range of dynamical balances to be considered short enough to neglect the variation in the phase

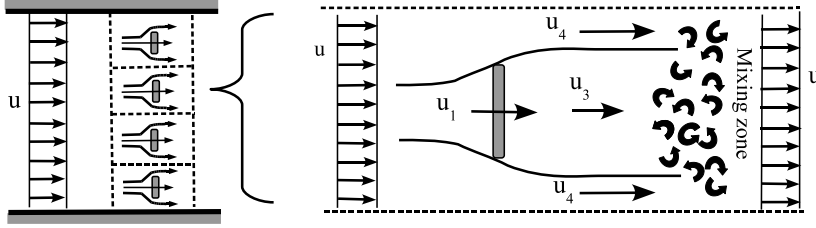


FIGURE 2. Schematic diagram of one row of turbines and one turbine within the row. Adjacent turbines create virtual walls, given by the horizontal dashed lines. These walls enhance the flow bypassing the turbines relative to the slower flows through the turbines, so that $u_4 \geq u > u_1 > u_3$.

and amplitude of the transport along a channel. Following GC05 (2.1) can be rewritten in terms of the transport $U(t) = u(x, t)/A(x)$ and integrated along the channel to give

$$\int_L \frac{dx}{A} \frac{\partial U}{\partial t} = -g[\eta_r - \eta_l] - \left[C_D \int_L \frac{dx}{hA^2} + \frac{1}{2} \left(\frac{1}{A_e^2} - \frac{1}{A_0^2} \right) + \sum^{N_R} \frac{C_{Ri}}{A_i^2} \right] |U|U \quad (2.2)$$

where η_l and η_r are the prescribed surface elevations at the ends of the channel, figure 1. The force due to each of the N_R turbine rows is $\rho C_{Ri} A_i |u_i| u_i$, where C_{Ri} is the drag coefficient of the i th row based on the channel's cross-sectional area at the row's location, A_i . $u_i = U/A_i$ is the free-stream velocity just upstream and downstream of the i th row of turbines. For simplicity the channel's area is assumed to be the same at both ends, i.e. A_0 . GC05 note that flow separation may result in a jet forming downstream of a constriction, which gives the term involving the areas A_e and A_0 , where A_e is the area of the jet as it exits the channel. If $A_e < A_0$ then there is a net loss of momentum from the channel which cannot be converted into power. Here there may be rows of turbines downstream of the constriction, figure 1. A jet impinging on any downstream rows will result in some turbines within a row generating more power and some less power. To keep the model simple it will be assumed that the constriction is gentle enough not to cause a separation and jet. Thus the exiting jet term will be discarded and the effects of a jet will be addressed in a future work.

The forcing by the water level difference between the ends can be expressed in the form $g(\eta_l - \eta_r) = a \sin(\omega t + \phi_g)$ where $a = g\eta_0 \Delta A_0/L$. V10 shows how to calculate Δ and ϕ_g . With this and non-dimensionalising time by $1/\omega$, x by L , areas by A_0 and by depths h_0 gives (2.2) in GC05's form

$$I \frac{\partial U'}{\partial t'} = \sin(t' + \phi_g) - \alpha [BC_D^* + C_F^*] |U'|U' \quad (2.3)$$

where $C_D^* = C_D L/h_0$ is the non-dimensional background bottom friction coefficient, $C_F^* = \sum C_{Ri}/A_i'^2$ is the farm's total non-dimensional drag coefficient and $\alpha = a/\omega^2 L A_0$. The geometric factors $I = \int_0^1 \frac{dx'}{A'}$ and $B = \int_0^1 \frac{dx'}{h' A'^2}$ are both ≥ 1 . Essentially (2.3) depends on total drag coefficient $\lambda = \alpha [BC_D^* + C_F^*]$, which is made up of two non-dimensional or rescaled drag coefficients. These are the effective background bottom drag coefficient $\lambda_0 = \alpha BC_D^*$ and the farm's gross drag coefficient $\lambda_T = \alpha C_F^* = \alpha \sum C_{Ri}/A_i'^2$.

The channel geometry used for all examples had rectangular cross-sections, either a uniform depth unconstricted channel or a uniform depth channel with a width constriction at its mid point. The constriction was modelled as a Gaussian curve with $0.2L$ between its points of inflection so that at $x = 0.2L$ and $0.8L$ the width is 99% of the

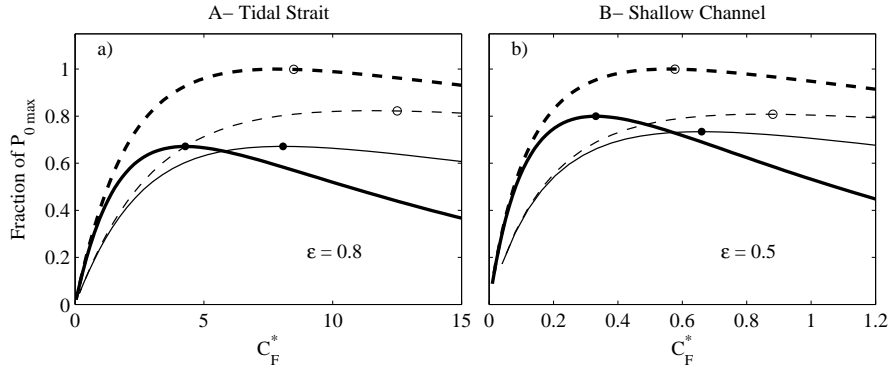


FIGURE 3. Power curves for a single row of turbines in the two hypothetical high flow channels of Table 1. Dashed curves are power lost to the turbines and solid curves the power available. Thick lines are for the channels without a constriction and thin lines are for the channels with a constriction reducing the width by 50%. Powers are relative to the potential of the un-constricted channel, \bar{P}_{0max} . Open circles give peak power lost, \bar{P}_{max} , at C_F^* . Solid dots show the maximum power available, \bar{P}_{avail} , at optimal tuning corresponding to C_F^{*opt} .

unconstricted width. The strength of the constriction is measured by the reduction in width at the narrowest section relative to the width at the ends. For brevity only width constrictions are discussed, though the model allows for depth constrictions due to a sill, which would preferentially enhance bottom friction in (2.2).

2.2. Drag coefficient of a single row of untuned turbines

The need for passage by vessels and marine life along a channel will necessitate gaps between turbines, figure 2. GC07 modeled turbines in a narrow channel where some flow is allowed to bypass the turbines through gaps within a row. This uniform water depth model assumed uniform steady flow upstream and downstream of the turbines and ignored bottom friction. Their results are expressed in terms of the fraction of the cross-sectional area taken up by the turbines, ϵ , and could be applied either to a single turbine or to many turbines within the same cross-section occupying a total fraction ϵ . The model also assumed that the gaps are large enough that the Froude number of the enhanced flow through the gaps is small, which restricts the model's applicability as $\epsilon \rightarrow 1$. For a farm consisting of multiple rows of turbines, it is also assumed that the spacing between rows is large enough to allow the enhanced flow bypassing the turbines in one row to fully mix with the retarded flow passing through the same turbines before encountering the next row.

By using Bernoulli and balancing mass and momentum within control volumes GC07 showed how the force on the turbines is related to the various velocities in figure 2. Using GC07's Eq. 2.8 the drag coefficient for a row of untuned turbines based on the channel's cross-sectional area can be written as

$$C_{Ri} = \frac{\epsilon_i}{2} (r_{4i}^2 - r_{3i}^2) \quad (2.4)$$

where $r_{ki} = u_{ki}/u_i$, $k = 1 \dots 4$, are the ratios of the various velocities near the turbine to the free-stream flow, figure 2 and ϵ_i is the fraction of the cross-section taken up by the i th row of turbines, i.e. its turbine density. The flow through the gaps between the turbines, u_{4i} (GC07 Equ. 2.23), can be rewritten

	A- Tidal Strait	B- Shallow Channel
Depth, h	100m	20m
Length, L	50km	2km
Width, W	10km	500m
Surface Phase Diff./Press. Grad. Phase, ϕ_η / ϕ_g	180° / 0°	10° / 275°
Tidal Amplitude, η_0 /Headloss amplitude, $\Delta\eta_0$	0.7m/1.4m	1.0m/0.17m
$\alpha/C_D^*/\lambda_0$	0.3/1.25/0.35	22/0.25/5.5
Peak power lost, no constriction, \bar{P}_{0max}	5.5GW	9.0MW
$C_{Fpeak}^*/\lambda_{Tpeak}$	7.8/2.3	0.56/12.5

TABLE 1. Two hypothetical examples of unconstricted high flow tidal channels. Both have semi-diurnal tides, $\beta = 1$, and $C_D = 0.0025$.

$$r_{4i} = \frac{1 - r_{3i} + \sqrt{\epsilon_i - 2\epsilon_i r_{3i} + (1 - \epsilon_i + \epsilon_i^2)r_{3i}^2}}{1 - \epsilon_i} \quad (2.5)$$

In addition the velocity passing through the turbines relative to the free stream can be expressed (GC07 Equ. 2.9) as

$$r_{1i} = \frac{r_{3i}(r_{4i} + r_{3i})}{r_{4i} + 2r_{3i} - 1} \quad (2.6)$$

GC07 also showed that the fraction r_1 of the power lost by the flow to the turbines is available for power production. So that for the multi-row farm here

$$\bar{P}_{lost} = \rho \sum^{N_R} C_{Ri} A_i \overline{|u_i|^3} \quad (2.7)$$

$$\bar{P}_{avail} = \rho \sum^{N_R} C_{Ri} A_i \overline{|u_i|^3} r_{1i} \quad (2.8)$$

where the over bar indicates an average over a tidal cycle. The difference between \bar{P}_{lost} and \bar{P}_{avail} is the energy dissipated as the fast bypassing flow mixes with the slower flow passing through the turbines. To maximise the power available the turbine through flow is adjusted, typically by adjusting the pitch of the turbine's blades. Here, as for the classic isolated turbine, the through flow ratio downstream of the turbines, r_3 , is chosen as a mathematically convenient tuning parameter. However, as the area of the wake downstream varies with turbine density, results will mostly be presented in terms of the flow fraction at the turbine r_1 . For the classic isolated optimal tuned Lanchester-Betz turbine $r_1 = 2/3$ and $r_3 = 1/3$.

2.3. Combined channel and turbine row model

The GC07 model for a row of turbines adapted in the previous section assumes steady flow and ignores bottom friction. To combine this with the channel model of Section 2.1 requires the assumption that each row takes up only a very short section of the channel. Consequently, within the rows the force of the turbines dominates bottom friction and flow inertia and the headloss across a row is in a quasi-steady state balance with the velocity. Outside of the rows bottom friction and inertia may still be significant. While the flow passing through one row is assumed to fully mix before encountering the next row, there is still an important interaction between rows. Reducing the tuning factor of any one row, r_{3i} , or increasing its turbine density, ϵ_i , increases the farm's total drag

coefficient in (2.3). This reduces the flow everywhere along the channel, affecting the power available from all rows.

To solve the combined model a set of ϵ_i and r_{3i} is used to calculate the farm's total drag coefficient, C_F^* . This is used in an approximate analytic solution to GC05's model equation (2.3) detailed in V10. The solution of the form $U' = U_0 \sin(t' + \phi_g - \phi_u)$ explains around 95% of the solution. Adapting the solution to a variable cross section channel gives

$$U_0 = \frac{\left(\sqrt{4\hat{\lambda}^2 + I^4} - I^2\right)^{\frac{1}{2}}}{\sqrt{2}\hat{\lambda}} \quad (2.9)$$

where $\hat{\lambda} = 8\lambda/3\pi$ and $\phi_u = \tan^{-1}(I/U_0\hat{\lambda})$. The analytic power curves are very similar to the numerical solution (not shown) in figure 3, with the analytical solution slightly overestimating the power lost, particularly in inertial channels. The analytic solution is preferred over the numerical solution as it greatly speeds the search to find a set of optimal tunings. Differentiating the analytic power lost gives an expression for the location of the peak power loss, C_{Fpeak}^* , which is too long to be useful, though there are simple exact peak locations for both the inertial and the steady state dynamical extremes. Fortuitously, C_{Fpeak}^* is approximately linear between the two dynamical extremes (as demonstrated by Karsten *et al.* (2008) for a channel connecting an ocean to a lagoon) so that

$$C_{Fpeak}^* \approx 2BC_D^* + \frac{3\pi\sqrt{2}}{8\alpha} I^2 \quad (2.10)$$

With the geometric factors and turbine parameters, α , C_D^* , r_{3i} and ϵ_i the solution to the channel model (2.3) can be used to give the average power lost and available in a single tidal cycle. The power available from the combined model is

$$\bar{P}_{avail} = \rho \overline{|U|^3} \sum_{N_R} \frac{C_{Ri} r_{1i}}{A_i^2} \quad (2.11)$$

For the approximate analytic solution $\overline{|U|^3} \approx 4U_0^3 a^3 / 3\pi\omega^3$. The set of tunings which maximises the power available, r_{3i}^{opt} , were found numerically using the simplex search method (Lagarias *et al.* 1998).

A measure of a farm's efficiency is the fraction of a channel's potential which is available for power generation. Thus a useful Farm Efficiency Index is

$$FEI = \frac{\bar{P}_{avail}}{\bar{P}_{max}} \quad (2.12)$$

The potential, \bar{P}_{max} , is the maximum average power that can be generated from the channel, given by the peak in the power lost curves in figure 3, and requires turbines to completely fill a channel's cross-section. Drag on turbine support structures and their electro-mechanical efficiency will reduce the fraction of a channel's potential which can be converted into electricity below (2.12).

The number of turbines is $N = \sum \epsilon_i A_i / A_T$, where A_T is the blade area of a single turbine, which can be expressed non-dimensionally as

$$N^* = \frac{N}{N_0} = \frac{1}{\min(A)} \sum_{N_R} \epsilon_i A_i \quad (2.13)$$

where $N_0 = \min(A) / A_T$ is the number of turbines required to completely fill the channel's smallest cross-section. Economic efficiency is related to the average output per turbine,

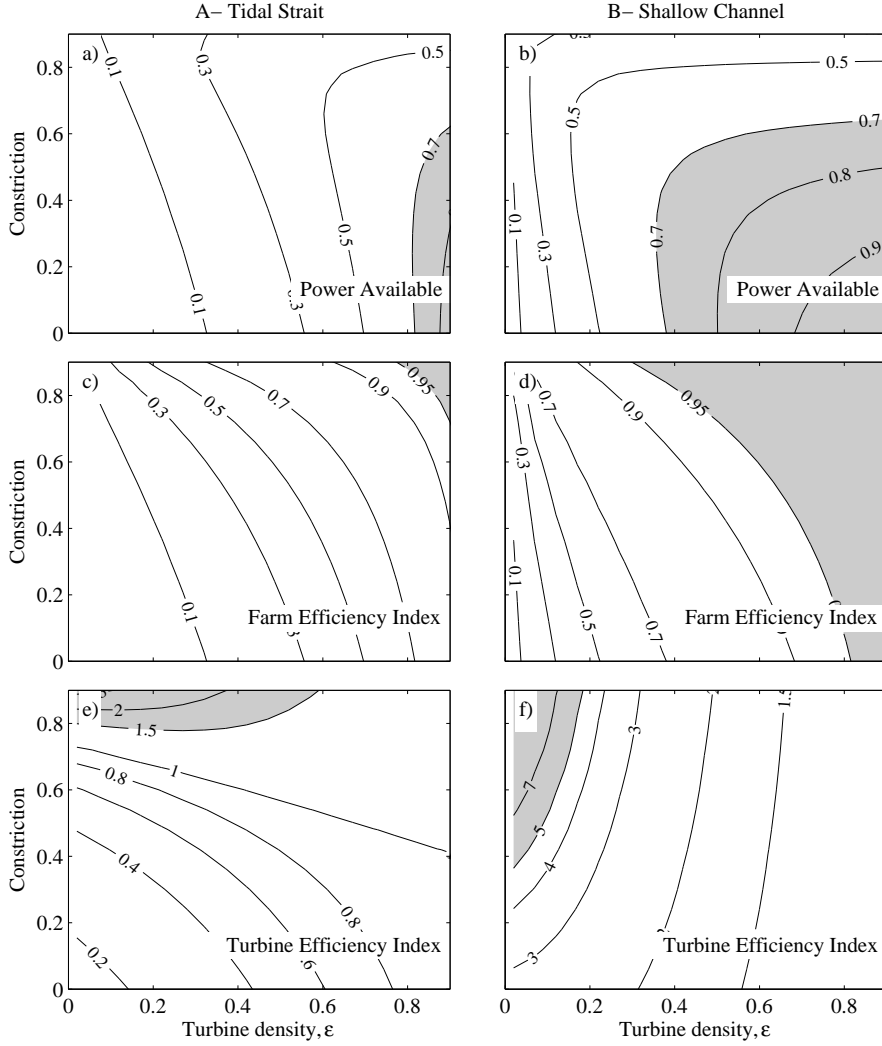


FIGURE 4. Power available and efficiency for a single row of optimally tuned turbines for a range of cross-sectional densities, ϵ and channel width constrictions. Top pair of plots are power available compared to unconstricted channel, $\bar{P}_{avail}/\bar{P}_{0max}$. Middle pair are the Farm Efficiency = $\bar{P}_{avail}/\bar{P}_{max}$. Lower pair give the Turbine Efficiency Index (2.14). Grey regions indicate high values.

which can be expressed as a Turbine Efficiency Index

$$TEI = \frac{\bar{P}_{avail}/N}{\bar{P}_{max}/N_0} = \frac{\bar{P}_{avail}}{\bar{P}_{max}N^*} \quad (2.14)$$

This has been normalised by the efficiency obtained by turbines completely filling the channel's smallest cross-section which generate the maximum possible power, i.e. the channel's potential \bar{P}_{max} . The TEI is similar to V10's "relative efficiency".

Two hypothetical examples of high flow channels were constructed to give representative values of the channel model parameters α and C_D^* , Table 1. The first is a 100 m deep tidal strait connecting two water bodies with semi-diurnal tides in anti-phase. The strait has a huge potential of $P_{0max} = 5.5GW$. \bar{P}_{0max} is given by the average power lost by

flow to the turbines at the peak in the power curves for an unstricted channel, figure 3. The second hypothetical channel is a shallow 20 m deep entrance to a large embayment and has a potential of $\bar{P}_{0max} = 9.0MW$.

The effective bottom drag coefficient $\lambda_0 = \alpha BC_D^*$ gives the importance of background bottom friction in (2.3). A large λ_0 implies a channel is in a quasi-steady state dynamical balance. Thus not only do high α and bottom drag coefficient contribute to making the dynamics of a channel quasi-steady state, constrictions also push a channel towards a quasi-steady state balance by increasing B . For the unstricted tidal strait $\lambda_0 = 0.35$, consequently flow inertia is significant to its dynamics. In contrast the shallow channel has $\lambda_0 = 5.5$ and its dynamical balance is a quasi-steady state with the velocity and pressure gradient almost in phase.

It is important to note that in the combined model ϵ_i takes on only discrete values which are integer multiples of A_T/A_i . Note also that the model cannot be used at very high ϵ_i without violating the assumption about the Froude number of the flow through the gaps, i.e. that $aU_0 r_{4i}/\omega A_i \sqrt{gh_i} \ll 1$. However, the need for navigation will generally restrict the ϵ_i to be sufficiently small that this Froude number condition is easily met.

There is also a tacit assumption in the combined model that any flow bypassing a turbine in the vertical plane is not accelerated by the proximity of the bottom or water's surface sufficiently to give rise to significant free surface effects. These are explored by Whelan *et al.* (2009) for closely horizontal spaced turbines forming a mid-water depth resistance strip. They found that blockage ratios above ≈ 0.5 can lead to an hydraulic jump and super-critical flows downstream of the turbines. In the combined model the horizontal gaps to allow for navigation are likely to be larger than the gaps between turbines and the free surface or bottom. Thus much of the flow is likely to bypass the turbine in the horizontal plane, reducing any free surface effects due to flow bypassing above and below the turbines. While avoiding significant free surface effects is partly covered by the requirement that the Froude number in the gaps is small, bypassing flow speeds are unlikely to be the same through the lateral and vertical gaps. Though it is not done here, there is a need for a more complete model to understand the speeds of bypassing flows around a turbine bounded between the bottom, free surface and adjacent turbines, e.g. an actuator disc in a rectangular domain.

3. Efficiency of a single row

figure 3 gives power curves for the two hypothetical examples in Table 1. A single row in the tidal strait requires a much higher density, $\epsilon = 0.8$ than a single row in the shallow channel, $\epsilon = 0.5$, to achieve high farm efficiency. The peaks of the curves of power available at optimal turbine tunings are shown by the solid dots at C_F^{*opt} corresponding to optimal tuning r_1^{opt} or r_3^{opt} . For all cases the farm's optimal drag coefficient C_F^{*opt} is slightly less than C_{Fpeak}^* , the location of the peak in the power lost curve. Consequently the optimal through flow fraction, r_1^{opt} , is higher than r_1 at the peak in the power lost curve. In the tidal strait a 50% constriction significantly reduces the power which can be lost to the turbines, yet the constricted strait has almost the same power available as the un-constricted strait. For the shallow channel the constricted channel has slightly less power available than the un-constricted channel.

The upper plots in figure 4 give the power available from a single row of optimally tuned turbines for a range of cross-sectional densities and width constrictions. Relative to an unconstrained channel, $\bar{P}_{avail}/\bar{P}_{0max}$, the power available is greatest when turbines almost fill an un-constricted channel. For both examples, at fixed smaller ϵ_i , increasing

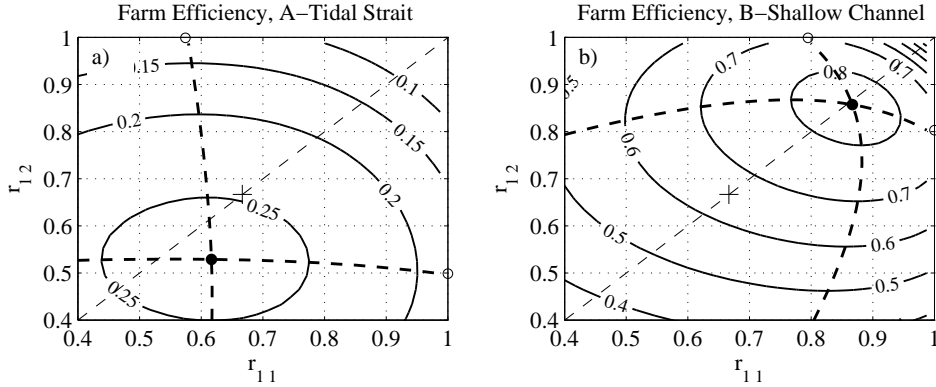


FIGURE 5. Effect of tuning on farm efficiency, $\bar{P}_{avail}/\bar{P}_{max}$, for a pair of rows in a channel with a 50% constriction. Axis are the r_{1i} of the two rows. The first row is in the constriction with $\epsilon = 0.2$ and the second is outside the constriction with $\epsilon = 0.5$. Thick dashed lines give optimal tunings for each row when the other's tuning is fixed. Black dot is global optimal tuning and open circles are optimal tunings in the absence of the other row. The thin diagonal dashed lines are $r_{11} = r_{12}$. The “+” gives $r_1 = 2/3$, the optimal tuning for the classic isolated Lanchester-Betz turbine.

the constriction initially increases the power available from fewer turbines. However for all ϵ strong constrictions reduce the power available by enhancing dissipation by bottom friction in the high flows through the narrowest cross-section. The middle plots of figure 4 give the farm efficiency, which is highest for high ϵ and strong constrictions. Increasing ϵ always increases farm efficiency, while the increase is more rapid for constricted channels. A consequence is that, for both examples at any given ϵ , fewer turbines are required to realise a larger fraction of a constricted channel's potential than for a similar unconstricted channel. For a given ϵ and constriction the shallow channel will realise a larger fraction of its potential, though in absolute terms the tidal strait has a far greater potential, Table 1.

The lower plots in figure 4 show that the power output per turbine, TEI (2.14), is greatest for a single turbine in a highly constricted channel. For the quasi-steady shallow channel adding turbines to the row always decreases the output per turbine. Surprisingly for the unconstricted or moderately constricted inertial tidal strait adding turbines to the row increases the output per turbine. Thus farms in moderately constricted inertial straits can have both the highest farm and turbine efficiency at the highest permissible ϵ . In highly constricted tidal straits the enhanced bottom friction pushes the strait towards a quasi-steady state balance, for which high turbine density is required to deliver a significant fraction of the potential, but there is a law of diminishing returns in the output per turbine as turbines are added to a row.

4. Tuning a pair of rows in-concert

The upper plots in figure 5 show the fraction of power available for a constricted channel with two rows. At maximum power available both the rows' optimal tunings (black dot) are higher than the optimal tunings they would have in the absence of the other row (open circles). Significantly greater power is available from the pair of rows from either acting alone. The figure demonstrates that to achieve the global maximum power available each row must be tuned in the presence of the other, i.e. in-concert.

In figure 5(a) or (b) the optimal tuning for the first row without the second is indicated

by the open circle along the top edge. Along this edge $r_{12} = 1$, turbines in the second row have feathered blades giving $C_{R2} = 0$, and thus generates no power. As r_{12} is decreased, the second row exerts some force on the flow and hence starts to generate power, sharing the load with the first row. Loading the second row increases the power available. However to maximise the total power available the optimal tuning of the first row (given by the near vertical dashed lines) must initially increase, which reduces its load. Conversely the optimal tuning of the second row also initially increases as the first row takes on some of the load. Thus it appears that in-concert optimal tuning of a row is higher than the optimal tuning it would have if they were the only row in the channel, as the total load of the finite resource is shared between rows.

The global optimal tunings for the row in the constriction, r_{11}^{opt} , are given in the upper plots of figure 6 for the two channel examples across a range of turbine densities. Optimal tunings, r_{1i}^{opt} , vary from $2/3$ in the lower left to near 1 in the other three corners, where turbines occupy most of the cross-section. r_{11}^{opt} for the shallow channel and r_{31}^{opt} (not shown) for both examples varies monotonically between the lower left and upper right. In contrast, for the tidal strait r_{11}^{opt} has a minimum around $\epsilon_1 = 0.3$ and $\epsilon_2 = 0$. Farm efficiency (not shown) varies from zero in the lower left of the plots and approaches 1 at the upper and right hand sides of the plots.

The difference between the optimal tunings of the two rows is given in the middle plots in figure 6. These illustrate the surprising result that, despite the constriction, there is no difference between the optimal tunings if both rows have the same turbine density. This occurs despite the row in the constriction having half the number of turbines in the other row. Furthermore, for the shallow channel over the full range of turbine densities the difference between the optimal tunings of the two rows is less than 5% of their mean tuning. Thus for the constricted shallow channel optimal tunings for the rows are almost the same over almost the full range of turbine densities. In contrast optimal tunings for the tidal strait differ by up to 20%. The contours in figure 6, derived from the more exact numerical solution, are very similar to those given for the approximate analytic solution, thus support the same conclusions.

The lower plots in figure 6 give the fraction of the total power generated by row 1 which lies in the constriction. For equal turbine densities, the narrower section generates 80% of the power. The rows make equal contributions along the 0.5 contour, which is displaced upwards due to the constriction. The lower contour plots for the two example channels appear identical, suggesting that the relative contribution of the two rows to the total power available is not dependent on the dynamical balance.

5. Multi-row farms

figure 7 gives an example of a channel with multiple rows of turbines where odd and even rows have different ϵ_i . figure 7(a) demonstrates that the more densely packed rows in the tidal strait have significantly lower optimal tunings than the less densely packed rows. Surprisingly, while the constriction raises all optimal tunings in the strait, optimal tunings for rows with the same ϵ appear to remain the same. For the shallow channel the tunings for all rows are almost the same, consistent with the two row example figure 6(d), with a constriction marginally increasing the near uniform optimal tunings. figure 7(b) shows the high density rows in the un-constricted tidal strait producing an order of magnitude larger fraction of the total power available than the lower density rows, despite the higher density being only twice the lower density. This suggests a strong bias towards the more efficient denser rows. In the constricted channel the row in the narrowest section, which also happens to have the higher density, produces almost 45% of the power available. This

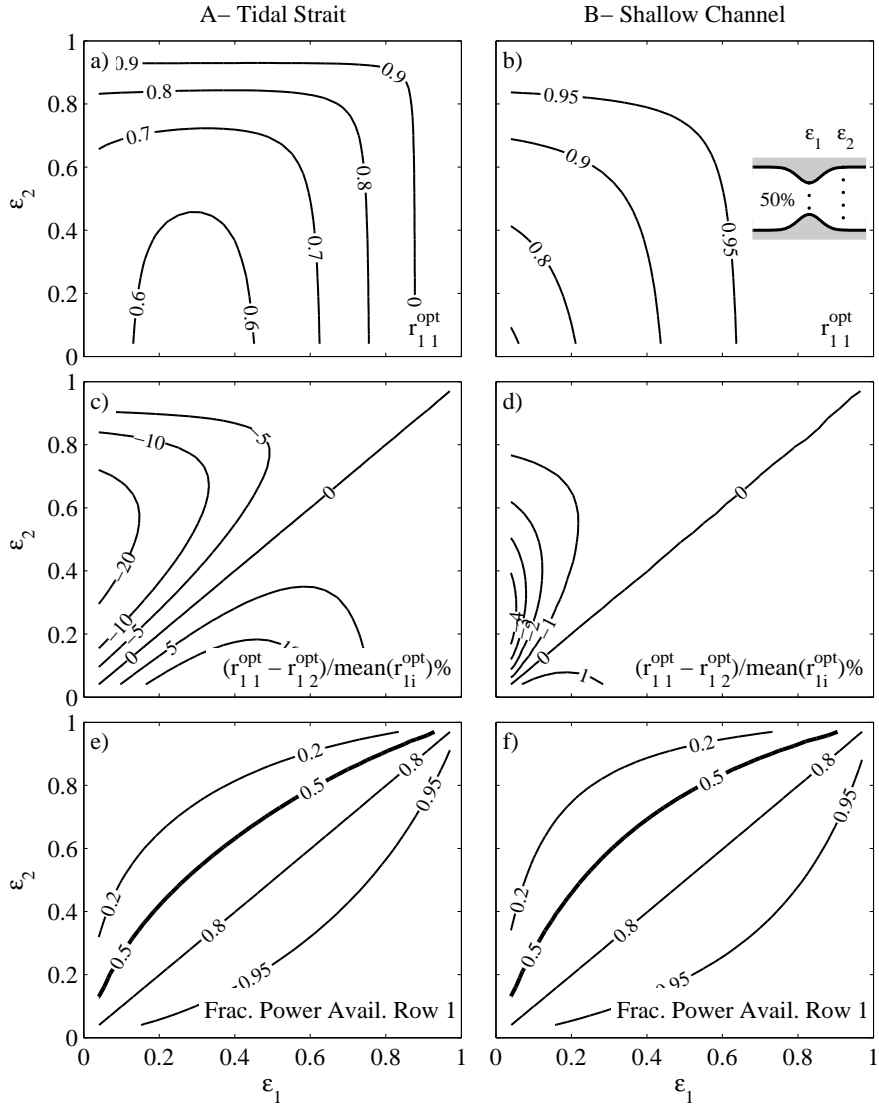


FIGURE 6. Optimal in-concert tunings for a pair of turbine rows in a channel with a 50% width constriction. Upper pair of plots give optimal tuning for row 1. Middle pair of plots are the difference between the optimal tunings of the two rows divided by the average optimal tuning as a percentage. Lower plots are the fraction of total power available generated by the first row.

indicates the bias of optimal tunings towards power production in the row within the more efficient constricted section. The fractions of power available for the shallow channel are also plotted in this figure, but the curves are almost indistinguishable from those of the strait. Other turbine densities and constrictions show the same. So it appears that the fraction of power available from each row is independent of the channel's dynamical balance, for fixed turbine densities and geometry.

figure 8 gives the fraction of potential realised by farms in the unconstricted hypothetical channels for given numbers of rows. The figure compares three tuning strategies, optimal in-concert tuning, using the optimal tuning for a single row alone in the channel

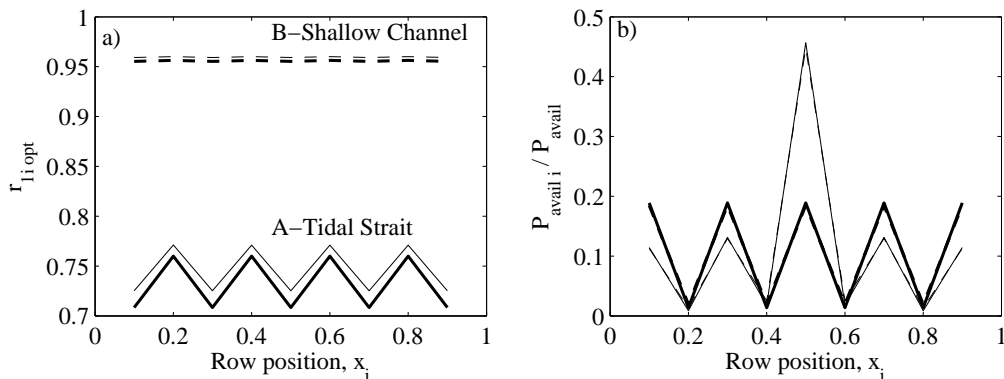


FIGURE 7. Variation along a channel of optimal tunings and power available for 9 rows of turbines. Odd rows have $\epsilon = 0.50$ and even rows $\epsilon = 0.25$. Solid lines are for the tidal strait example and dashed lines the shallow channel. Thick lines are for an unconstricted channel and thin lines a channel with a 50% width constriction. a) Optimal tuning. b) Fraction of power available from each row.

(OTSRA) and the classic Lanchester-Betz tuning. For both turbine densities the differences between strategies become significant when realising more than 50% of a channel's potential, with in-concert tunings giving significantly higher farm efficiencies than the other two strategies. For the shallow channel the differences between strategies also becomes apparent when realising more than 50%, though far fewer rows are required to achieve this. The difference between strategies is larger at moderate turbine densities with in-concert tuning delivering much more power for larger numbers of rows or at higher densities. Optimal in-concert tunings (not shown) increase from $r_3 \approx 1/3$ for one row to 0.55 and 0.82 in the tidal strait with 80 rows for cases of $\epsilon = 0.1$ and 0.25, respectively, and increase to 0.76 and 0.91 for 15 rows in the shallow channel. The increase in optimal in-concert tuning shares the load of generation from a finite resource across more rows, though there is a diminishing return on new rows. If enough rows are added, then the power available curves of the other two strategies peak, then decline. Only for in-concert tuning does the power available continue to increase as rows are added, albeit with a diminishing return. Thus tuning in-concert is required to realise most of a channels potential.

6. Inferences about optimal in-concert tunings

The optimal tuning for a particular row can be found by setting the partial derivative of the power available (2.11) with respect to the tuning parameter of that row to zero, while keeping the tunings of the other rows constant. For this discussion the flow fraction at the turbine will be used as the tuning parameter as it appears in (2.11). Thus the optimal tuning for the k th row can be expressed as the solution to the equation

$$r_{1k} - \left[\left(\frac{-1}{C_{Fk}} \frac{\partial C_{Fk}}{\partial r_{1k}} \right)^{-1} \right] = \left\{ \frac{-\alpha}{|U|^3} \frac{\partial |U|^3}{\partial \lambda} \sum_{i=1}^{N_R} \frac{r_{1i} C_{Ri}}{A_i'^2} \right\} \quad (6.1)$$

The global optimal tuning is the set of r_{1k} which simultaneously solves all N_R non-linear equations. Though these equations are too complicated to solve, several inferences about optimal tunings can be made from their structure. It should be noted that the factor due to the area of the k th row, $1/A_k'^2$, was common to all terms and canceled out, thus A_k'

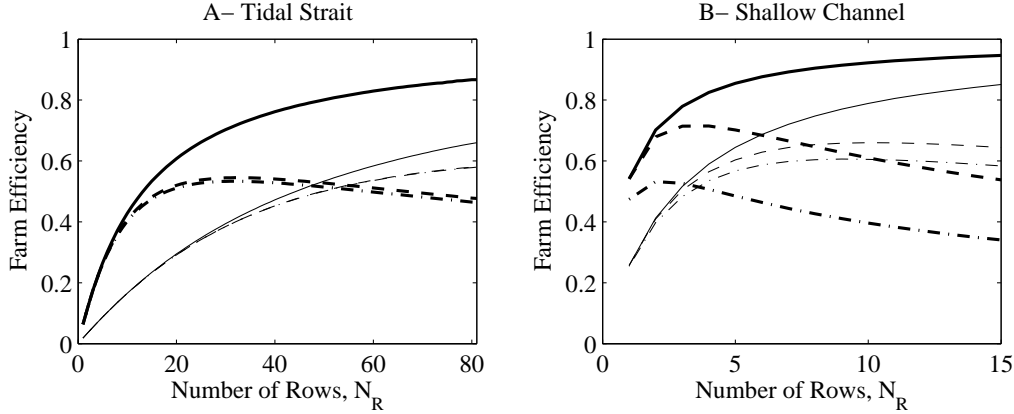


FIGURE 8. Farm efficiency for three tuning strategies for a farm with an increasing number of rows in an unstricted channel. Thick lines are for $\epsilon = 0.25$ and thin lines are for $\epsilon = 0.1$. Solid lines are for rows tuned in-concert, dashed lines are for turbines tuned to the optimal tuning of a single row alone in the channel, OTSRA. The chain dashed lines are for the Lanchester-Betz optimal tuning of $r_3 = 1/3$.

does not appear explicitly in the equation. Also note that the $\{ \}$ term is the same for all equations, i.e. row invariant.

6.1. *In both constricted and unstricted channels, rows with the same turbine density have the same optimal tuning*

From section 2.2 the $\{ \}$ bracketed term can conceptually be expressed as depending only on two variables, (ϵ_k, r_{1k}) . Thus for all rows equation (6.1) can be expressed conceptually as the same function of three variables

$$\mathcal{F} \left(\left\{ \frac{-\alpha}{|U|^3} \frac{\partial |U|^3}{\partial \lambda} \sum_{i=1}^{N_R} \frac{r_{1i} C_{Ri}}{A_i'^2} \right\}, \epsilon_k, r_{1k} \right) = 0, \quad k = 1 \dots N_R \quad (6.2)$$

The r_{1k}^{opt} which solve these equations depend only on the other two variables. The first of these, the $\{ \}$ bracketed term, is the same for all equations/rows, thus any functional difference between the equations for each row is entirely due to the second variable ϵ_k . Thus equations/rows with the same ϵ_k will yield the same solution for r_{1k}^{opt} . Consequently the first inference is that, in both constricted and unstricted channels, rows with the same turbine density have the same optimal tuning. The optimal tunings for the two row examples in figure 6(c) and (d) demonstrate this, where for this constricted example there is no difference in the optimal tunings when the densities are equal. figure 7 also confirms this, where a 50% constriction shifts the tunings upwards but alternate rows with the same ϵ still have the same optimal tuning, even though rows in the narrower sections produce much more power.

6.2. *In both constricted and unstricted channels the optimal tunings of all rows are almost equal at “high” ϵ , even if turbine densities vary significantly*

The second inference is more subtle. In (6.1) if the $\{ \}$ bracket term is only weakly dependent on ϵ or small then r_{1k}^{opt} depends mostly on the row invariant term $\{ \}$. Thus when $\{ \}$ is weakly dependent on ϵ , or small, the optimal tuning will be almost the same for all rows, i.e. tunings are near uniform, even if turbine densities or cross-sectional areas are significantly different. figure 9 plots the size of $\{ \}$ and demonstrates that for

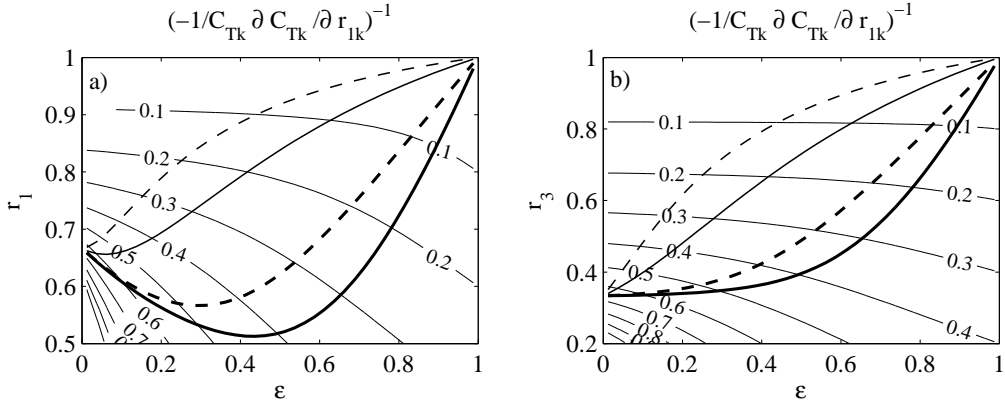


FIGURE 9. Contours of the $[-]$ term in (6.1) a) As a function of ϵ and r_1 . b) As a function of ϵ and r_3 . The curves give optimal tunings for a single row of turbines for the two examples in Table 1. The thick solid lines are for the tidal strait and the thin solid lines are for the shallow channel. The dashed lines are for the same examples with a 50% width constriction.

$r_1 > 0.85$ and $r_3 > 0.6$ the term varies little with ϵ and is relatively small. Thus at these high tunings, optimal tunings will be approximately the same for all rows, even in highly constricted channels. Several circumstances lead to high optimal tunings. Firstly if $\epsilon \rightarrow 1$ then $r_{1k}^{opt}, r_{3k}^{opt} \rightarrow 1$. Figures 6 and 9 show the quasi-steady state shallow channel example typically has higher optimal tunings than the inertial tidal strait at the same ϵ . Thus steady state channels reach uniform tunings at much lower ϵ values than inertial channels. In addition for both examples optimal tunings converge on the classic Lanchester-Betz tuning of $r_{1k}^{opt} = 2/3$ when all rows have very low turbine densities. The two row example in figure 6 clearly shows this, where the difference between the the tunings of the two rows in the inertial strait varying by more than 20% when combining a medium density row with a very low density row. This example also shows that $\epsilon_1 > 0.8$ or $\epsilon_2 > 0.9$ are required to give differences of less than 5%. In contrast the variation of the difference in optimal tunings for the shallow channel is an order of magnitude smaller and near uniformity of optimal tuning occurs at very low turbine densities, with differences less than 5% over almost the full range of the ϵ_i . Thus almost any density in the shallow channel would be considered “high” and thus quasi-steady channels will typically have near uniform optimal tunings.

Note that in figure 8 and figure 9 a constriction increases optimal tunings, i.e. reduces C_{Rk} . However the power curves in figure 3 show that constrictions require a higher total drag coefficient C_F^* to maximise power available. This demonstrates that the effect of area, $1/A_k^2$, due to the constriction has a greater influence on C_F^* than does the tuning, r_{1k}^{opt} , via C_{Rk} . Thus, counterintuitively, a constriction increases optimal tunings, making optimal tunings more uniform within the channel, while also pushing a channel closer to quasi-steady state dynamical balance.

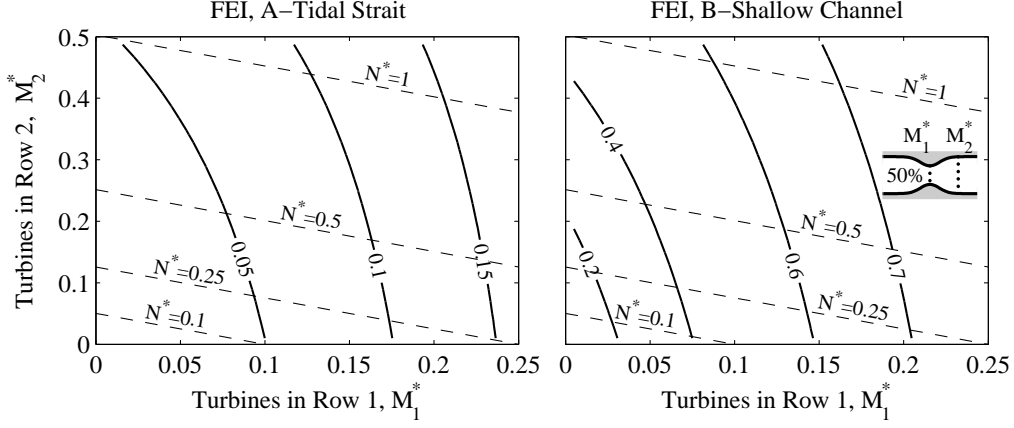


FIGURE 10. Farm efficiency, $FEI = \bar{P}_{avail}/\bar{P}_{max}$ for a channel with 50% width constriction and two rows of turbines. First row is in the narrowest cross-section and the second row outside the constriction. Dashed lines indicate where total number of turbines, N^* , equals given values.

6.3. *At optimal tuning rows with the same ϵ contribute a proportion of the total power available which depends only on $1/A_k^2$*

This third inference follows directly from the first. From (2.11) the fraction of power available from the k th row at optimal tuning is

$$\frac{C_{Rk} r_{1k}^{opt} / A_k^2}{\sum_{i=1}^{N_R} C_{Ri} r_{1i}^{opt} / A_i^2} \quad (6.3)$$

The first inference shows that at optimal tuning two rows with the same ϵ have the same r_{1k}^{opt} . As C_{Rk} depends only on ϵ_k and r_{1k}^{opt} , at optimal tuning the product in the numerator, $C_{Rk} r_{1k}^{opt}$, will be the same for rows with the same density. Consequently the relative contribution to total power available for rows with the same density is determined entirely by the factor $1/A_k^2$. figure 7(b) confirms this where, for an unconstricted inertial channel, rows with the same density deliver the same fraction of the total power available. In the constricted inertial strait the row in the constriction contributes the most power, with that in the narrowest section contributing four times that of the end rows, which are outside the 50% constriction. The lower plots in figure 6 also demonstrate this where at equal ϵ the relative contributions of the two rows, with one in the 50% constriction and one outside the constriction, should be 4 : 1, or 80% from the first row.

The lower plots in figure 6 and figure 7(b) demonstrated that, for fixed ϵ_i and geometry, the fraction of power available from each row was the same for both hypothetical examples, i.e. independent of the channel's dynamical balance. There does not appear to be a simple way to infer this from (6.3) as, although a row may have the same A_k and ϵ_k in both example channels, optimal tunings and C_{Rk} for the row will be very different in the two examples.

7. Farms Constrained by maximum density and turbine numbers

While navigational requirements will constrain the maximum number of evenly spaced turbines per row, economics will constrain the total number of turbines in a farm. figure 10 gives the fraction of power available at optimal tuning as a function of the number

of turbines in each row, $M_i^* = M_i/N_0$. In this example it is assumed that navigational constraints restrict $M_i^* \leq 0.25$. The dashed lines give combinations of the M_i which give the same total number of turbines. For all cases farm efficiency is highest at the righthand end of the line. Thus for $N^* \leq 0.25$ the optimal configuration is to put all the turbines in the row within the constriction. If larger numbers are economically feasible then the second row can be progressively filled, while still ensuring no more than 25% of either cross-section is taken up by turbines. Thus the best strategy for growing a farm appears to be the intuitive one: fill the most efficient cross-section first, followed by the next most efficient section.

8. Conclusions

The necessity to tune rows of turbines in-concert arises out of an interaction between rows within a short narrow channel. This interaction results from the tuning of individual rows affecting the flow through all rows. The surprise is that in several circumstances the optimal in-concert tunings are the same or almost the same. Firstly, optimal tunings are the same for rows with the same turbine density, ϵ , even in constricted channels. Secondly any effect which results in higher optimal tunings makes these optimal tunings more uniform between rows even if turbine densities or cross-sectional areas differ. Channels which are in a quasi-steady dynamical balance typically have higher optimal tunings and thus rows have almost equal optimal tunings for most combinations of turbine densities. Constrictions push the dynamical balance towards a quasi-steady one, requiring higher optimal tunings and thus also making optimal tunings more uniform. Adding rows, which spreads the load of the finite resource across more turbines, increases optimal tunings and hence also makes those tunings more uniform between rows.

The results suggest that optimal tunings preferentially load the most efficient row, e.g. figure 7(b), thus a useful concept to introduce is that of the most efficient row i.e. MER. This is not necessarily the row in the narrowest cross-section, but the row with the combination of the degree of constriction at the row's location and maximum permissible turbine density which has the highest efficiency, as indicated by figure 4(c) and (d).

The fluid dynamics also has significant implications for the economics of farm development. Firstly, if numbers of turbines are limited then farms should grow by filling the MER up to the maximum permitted by any restriction on ϵ , before turbines are placed in less efficient cross-sections. Secondly, in quasi-steady state channels, the return per turbine reduces as the farm takes up more of the cross-section. Thus quasi-steady channels, either shallow channels or tidal straits with strong constrictions, exhibit a law of diminishing return per turbine, with turbines becoming less efficient as farm efficiency grows. However in inertial straits with moderate or no constriction, the output per turbine increases as the farm takes up more of the cross-section, making both the turbines and the farm more efficient. Thus not only do large tidal straits have a huge potential, the economics of realising the potential of some straits is much better than quasi-steady state channels. For both examples, once maximum permissible ϵ_i have been achieved, figure 8 demonstrates that there is always a diminishing return on rows added to a farm.

A secondary aim of this work was to provide understanding for developers using 2D and 3D hydrodynamic models to assess a site's ability to produce power. These models will require idealised turbines and, when necessarily densely packed to realise a large fraction of a channel's potential, these turbines must be tuned in-concert. This may require searching an N dimensional tuning space, which may be computationally prohibitive for large farms. Several results presented here may make this optimisation more feasible. For equal density rows, or those in a quasi-steady state channel, optimal tunings are the same

or nearly the same. Thus for these cases, assuming the idealised turbines have the same tuning, reducing the tuning space to one dimension may give near optimal power available. Even in inertial channels with unequal turbine densities, it may still make sense to take equal tunings as a starting point to speed the more exhaustive search for the global optimum. A future work will focus on strategies to get close enough to the global optima within the multi-dimensional tuning space that any further improvement is small.

Comments and editing by Craig Stevens and the students of the Ocean Physics Group were much appreciated.

REFERENCES

- BETZ, A. 1920 Das Maximum der theoretisch möglichen Ausnutzung des Windes durch Windmotoren. *Gesamte Turbinenwesen* **17**, 307–309.
- GARRETT, C. & CUMMINS, P. 2005 The power potential of tidal currents in channels. *Proc. Royal Society A* **461**, 2563–2572.
- GARRETT, C. & CUMMINS, P. 2007 The efficiency of a turbine in a tidal channel. *Journal of Fluid Mechanics* **588**, 243–251.
- KARSTEN, RH, McMILLAN, JM, LICKLEY, MJ & HAYNES, RD 2008 Assessment of tidal current energy in the Minas Passage, Bay of Fundy. *Proceedings of the I MECH E Part A Journal of Power and Energy* **222** (5), 493–507.
- LAGARIAS, J. C., REEDS, J. A., WRIGHT, M. H. & WRIGHT, P. E. 1998 Convergence properties of the Nelder-Mead simplex method in low dimensions. *SIAM J. of Optimization* **9** (1), 112–147.
- LANCHESTER, F. W. 1915 A contribution to the theory of propulsion and the screw propeller. *Trans., Inst. Naval Archit.* **LVII**, 98–116.
- SUTHERLAND, G., FOREMAN, M. & GARRETT, C. 2007 Tidal current energy assessment for Johnstone Strait, Vancouver Island. *Proceedings of the Institution of Mechanical Engineers, Part A: Journal of Power and Energy* **221** (2), 147–157.
- VENNELL, R. 1998 Oscillating barotropic currents along short channels. *Journal of Physical Oceanography* **28** (8), 1561–1569.
- VENNELL, R. 2010 Tuning turbines in a tidal channel. *Journal of Fluid Mechanics* **663**, 253–267.
- WHELAN, J. I., GRAHAM, J. M. R & PEIR, J. 2009 A free-surface and blockage correction for tidal turbines. *Journal of Fluid Mechanics* **624**, 281–291.